

*SURFACE CONJUGATION OF
UPCONVERSION NANOPARTICLES VIA
SUPRAMOLECULAR HOST-GUEST SELF-
ASSEMBLY*



Yulong Sun

Supervised by

Dr Joshua Chou (Principal Supervisor)

Dr Xiaoxue Xu (Co-Supervisor)

A/Prof Alison T Ung (Co-Supervisor)

School of Life Sciences

Faculty of Science

University of Technology Sydney

This dissertation is submitted for the degree of Doctor of Philosophy

December 2018

In loving memory of my grandfather, Mr. Jingzhi Fu (1937-2017)

To my grandmother, my mother, my father, and all of friends

CERTIFICATE OF ORIGINAL AUTHORSHIP

I, Yulong Sun declare that this thesis, is submitted in fulfilment of the requirements for the award of Doctor of Philosophy, in the School of Life Sciences, Faculty of Science at the University of Technology Sydney.

This thesis is wholly my own work unless otherwise reference or acknowledged. In addition, I certify that all information sources and literature used are indicated in the thesis.

Yulong Sun

Signature: _____
Production Note:
Signature removed prior to publication.

Date: 30 August 2018

ABSTRACT

Surface Conjugation of Upconversion Nanoparticles *via* Supramolecular Host-Guest Self-Assembly

Yulong Sun

Surface functionalization and conjugation hold the key to driving many purpose-synthesized nanoparticles into real-world applications. Lanthanide (Ln) ions doped upconversion nanoparticle (UCNP) is a good example: while it delivers a great promise as molecular probes, sensors, drug carriers and light transducers for a library of application in the area of biological and physical science. However, the hydrophobic surface of UCNPs, sometimes, is one of the main challenges for further applications, especially in natural science. It remains a bottleneck for the community to explore practical strategies to functionalize the UCNPs surfaces for hydrophilicity conversion and further bioconjugation to meet many cellular and molecular specific needs.

Supramolecular self-assembly is one of the leading topics in supramolecular chemistry. It is a process in which disordered molecular building blocks are specifically re-ordered and also a phenomenon where the components of a system assemble themselves spontaneously *via* interaction to form a larger functional unit. In the view of thermodynamics, self-assembly is an equilibrium process where the assembled components are in equilibrium with the individual components. In other words, it is driven by the minimization of Gibbs free energy. Compared with molecular chemistry, self-assembly, as the most critical component of the assembled method, was formed by intermolecular forces.

This thesis shows a new surface conjugation approach for UCNP modification *via* supramolecular host-guest interactions leading as-made oleic acid (OA) stabilized UCNPs (OA-UCNPs) from hydrophobic into hydrophilic. At the same time, the modified

host molecules on the surface of UCNPs can provide a considerable number of cavities, which can form the host-guest interaction with a series of molecules, such as anti-cancer drugs, biomolecules, and inorganic materials. The advantage of the modification approach is no further reaction formed for conjugation, which hugely increases the binding amounts and also shows the excellent binding behaviour by using the different binding systems.

This thesis is aiming to conduct studies of:

- (i) the investigation of the surface of OA-UCNPs (in **Chapter 3**)

To convert UCNPs with high efficiency and yield, the original cover needs to be investigated. We predict and proof the binding strength and binding mode between an OA and two β -NaYF₄ crystal surfaces of UCNPs.

- (ii) the binding behaviours of different organically functional groups (**Chapter 4**)

Compared with the original of OA from the surface of UCNPs, we also choose several organic molecules which hold different functional groups. We discuss the effect of different functional groups and, most importantly, the binding mode and binding behaviour on the surface of UCNPs.

- (iii) the investigation of binding behaviours of macrocycles on the surface of UCNPs and their applications in binding with organic molecules, biomolecules, and inorganic materials (**Chapter 4 ~ Chapter 6**).

We raise and design a new approach to convert the surface of UCNPs with different kinds of macrocycles. Then, we provide three applications in the areas of drug delivery, cell targeting, and energy transfer.

The thesis is organized as follows:

There are four main parts of the thesis, which includes:

- **Part I** Background

In this part, I introduce some basic information about supramolecular chemistry and UCNPs. The section of supramolecular chemistry consists of the concepts of supramolecular chemistry, supramolecular interactions, the selectivity of supramolecular chemistry, host-guest chemistry, self-assembly, and the current development of supramolecular chemistry. In the section of UCNPs, I start from the mechanism of upconversion to show the advantage of the upconversion materials, then display the synthetic methods of UCNPs for the further discussion on the surface modifications.

- **Part II** Literature Review: the surface modification and conjugation of UCNPs.

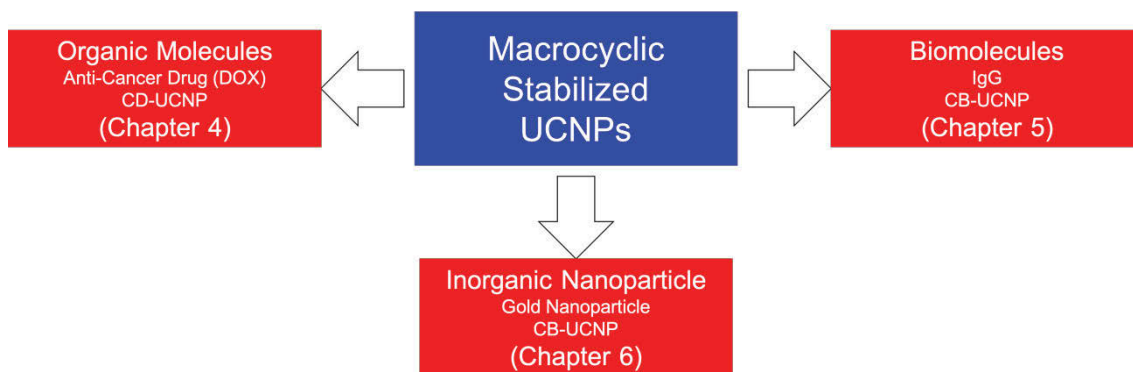
In this part, the surface modified approaches are sorted by the different supramolecular interactions. Except for the surface modification criteria, this review also gives a summary of surface conjugation of UCNP *via* supramolecular interactions with organic molecules and inorganic nanoparticles.

- **Part III** The original surface of OA-UCNPs

This part shows the synthesis and characterization of OA-UCNPs, and also the binding behaviour of OA on two kind crystal surfaces of UCNPs. This part also provides significant evidence to increase the efficiency of ligand exchange and surface binding.

- **Part IV** The applications of macrocycles modified UCNPs

This part includes three kinds of applications: molecular conjugation, biomolecular conjugation, and inorganic nanoparticle conjugation. All of these designs are based on the supramolecular host-guest interactions. In these chapters, we use two kinds of macrocycle to modify the surface of UCNPs for conjugating different types of organic molecules or inorganic materials, which showed in the following figure.



In **Chapter 4**, we conjugate anti-cancer drug, Doxorubicin Hydrochlorate (DOX), on the surface of UCNPs to test the bioavailability of DOX-loaded cyclodextrin-stabilized UCNPs (CD-UCNP). **Chapter 5** shows the binding properties of cucurbit[7]uril-stabilized UCNPs (CB-UCNP) with biomolecules, Immunoglobulin G, for cell targeting. The physical effect of UCNPs with AuNPs is investigated by the same binding approach, which explained in **Chapter 6**.

ACKNOWLEDGEMENTS

First of all, I would like to thank my great family: My grandfather, Mr Jingzhi Fu (1937-2017), for always setting an example for me and telling me how to be a good person. I still keep the letters he wrote to me over the years. These letters are not only encouragement but also a kind of care for me; My grandmother, Mrs Huang, for giving me all her love and parenting. She is the most important person in my life; My mother for her understanding and support. In those days, when I had to face difficult choices, she was the only one who had always supported and encouraged me; and My father for his silently guarding. Thank you so much for their support and encouragement over the past 30 years. They give me all their love but never ask for anything.

In my hometown, I spent 18 years finishing all my educations from elementary school to high school. Thanks all my teachers, who include Mrs Liu, Mr Li, Mrs Zhang, for not only teaching me knowledge but also telling us how to get along with others.

In Harbin, my second hometown, I spent four years getting my bachelor's degrees in engineering and management. I really appreciate all the faculty and staff from Department of Pharmaceutical Engineering for giving the knowledge and taking me into the world of science. Especially, I would like to offer my special thanks to Prof Hongrui Ji and Prof Miao Sun for giving me the great support on my Ph.D. application; Mrs Xizhi Zhao for taking me to the world of organic synthesis. Also, I would like to thank all of my friends in my University, Fujing Liu, Yong Zhao, Shikan Yang for the great support in that four years.

At Jilin University, I would like to thank Prof Yingwei Yang and Prof Sean Zhang for their professional guidance and valuable suggestion in science. I would also like to extend my thanks to these people for the collaboration and contribution to my research: Prof Minjie Li, Dr Bingjie Yang, Guojie Liu, Dr Yue Zhou, Dr Qinglan Li, Dr Yanqiu Wang,

Daxiong Chen, and Yuanchao Lv. Also, I would like to thank Dr Guan Wang, Dr Chu Wang, and Dr Gong Xin from College of Life Sciences for the great collaboration of my project. Special thanks to Ms Yanfang Sun for the unforgettable and enjoyable cooperation on the polymer project. I would also like to extend my thanks to the technicians of the laboratory for their help in offering me the resources in running the program.

At Northwestern University, I would like to give my highest respect to Sir Fraser Stoddart for giving me a chance for joining his group and also for the patient guidance and enthusiastic encouragement. Besides, I would like to thank Dr Dennis Cao for giving me a great help when I arrived Evanston, and Dr Alyssa Avestro for helping me polish my writing and teaching me how to prepare my presentation slides. Then I want to thank my office mate, Dr Yuping Wang for introducing many friends to me, by the way, he is also my lunch mate at that time. Dr Yilei Wu for taking me to the city of Chicago and introducing me to many Italian cultures.

At Tsinghua University, I would like to express my great appreciation to my research mentor, Prof Hongyu Zhang. That was the darkest time when I joined his group. He gave me a lot of support and made me regain my confidence. That was also a good experience that I learned a lot of knowledge of tribology from him, which gave me a new direction for future research. Besides, I would like to thank the whole group, Yanfang Sun, Tao Sun, Yi Wang, Yixin Wang, Xiaolong Tan, Yiwei Zheng, Ke Ren, Peng Zhao, Sizhe Liu, Dr Mingrui He, Dr Xiuling Ji, Kuan Zhang, Yaoyu Jiao, Ying Han, and Li Wan.

In 2015, I moved to Sydney and started my new journey in UTS. First of all, I would like to express my great appreciation to my supervisors, Dr Joshua Chou, Dr Helen Xu, and Prof Alison Ung. Thank Josh for the opportunities that he has created for me, as well as his patience and guidance in my darkest time. Thank Helen for bringing me to the world of crystal chemistry, allowing me to comprehend material science from a more

microscopic perspective. And also thank Alison for the great help on organic chemistry. More importantly, every time I chat with Alison, I have a feeling at home. I am very fortunate to have these three as my supervisors. In these few years, they are more than just my supervisors, more like my best friend.

Much of the work described in this thesis cannot be completed so smoothly without the help of the kind people around me in the lab: Dr Wenjing Zhang for the great support on nanoparticles; Dr Joshua Chou for helping and teaching me on cell study; Baoming Wang for the cell imaging test and warm discussion; Dr Helen Xu for the material analysis and characterization; Yingzhu Zhou for the optical test; and Dr Olga Shimoni for the analysis of protein conjugation. Besides, I would like to thank my lab mates, Jiayan Liao, Bo Shao, Alex Gee, Matthew Cappadona, Christian Clarke, and Iurii Bodachivskyi for the support and encouragement. I also would like to thank all the members from Advanced Tissue Regeneration & Drug Delivery Group and Institute for Biomedical Materials and Devices for their great suggestion and discussion: Prof Dayong Jin, Dr Fan Wang, Dr Jinghua Fang, Dr Lu Liu, Zhiguang Zhou, Ming Guan, Chao Mi, Hao He, Dr Ying Wang, Anantdeep Kaur, Huan Wu, Yuan Liu, Dr Peter Su, Dr Laixu Gao, Guochen Bao, and Dr Joris Goudsmits. I am particularly grateful for the lab and technical assistance given by Dr Linda Xiao, Dr Ronald Shimmon, and Katie McBean.

In addition, I would like to thank my friends when I live in Sydney: Sheran Li, a knowledgeable person, for her warm sharing, great help and useful suggestions; Steven Vasilescu, my first Australian friend, for teaching me many useful English words which we could not learn from textbook; Jen Ming and Shilun Feng, the cute couple, for their positive life style; Jim Li, the non-economically suitable warm man, for his kindness, sharpness, and helpfulness; Wenjing Zhang, the sunflower, for bringing us the joy and special brain circuit; Yingzhu Zhou and Baoming Wang in “3A on the way” group for their help, encouragement and support in those days; Yibin Wei and Xiaoteng Jia in

“Sausage BBQ” group for our unlimited chat and alcohol; Mehran Kianinia, Yan Wang and Xin Xu, the Gold Coast group, for the unforgettable seaside Spring Festival; Penny Fang, the live map of Sydney, for her delicious chicken legs and food recommendations that won’t let you down; Yameng Zheng, an emotional person, for taking in her luxuriously configured office; and Zhengnan Shan, a person who never gets drunk, for his courtesy and humility.

Finally, I would like to thank all the people who appeared or will appear in my life. Thank you so much for telling me how the world is and how to enjoy the life.

Yulong Sun

City Campus, UTS

28 August 2018

CONTENTS

1 WHEN SUPRAMOLECULAR CHEMISTRY MEETS UPCONVERSION NANOPARTICLES: MAJOR CONCEPTS OF SUPRAMOLECULAR CHEMISTRY AND UPCONVERSION NANOPARTICLES	1
1.1 WHAT IS SUPRAMOLECULAR CHEMISTRY?.....	2
1.2 SUPRAMOLECULAR INTERACTIONS	6
1.2.1 Ionic and Dipolar Interactions	7
1.2.2 Hydrogen Bond	8
1.2.3 π -Interactions	10
1.2.4 van der Waals Force	11
1.2.5 Hydrophobic Effects.....	11
1.3 SELECTIVITY	12
1.3.1 The Mechanism and Factors of Selectivity	13
1.3.2 Binding Constants	15
1.3.3 Kinetic and Thermodynamic Selectivity.....	17
1.3.4 Solvent Effect.....	17
1.4 HOST-GUEST CHEMISTRY	18
1.4.1 Guest	18
1.4.2 Hosts-Macrocycles.....	18
1.5 SELF-ASSEMBLY	24
1.6 MECHANICALLY INTERLOCKED MOLECULES (MIM)	25
1.6.1 Rotaxanes and Pseudorotaxanes	25
1.6.2 Catenanes.....	26
1.7 MOLECULAR MACHINE	27
1.8 INTRODUCTION OF UCNPs.....	28
1.8.1 Mechanism of Upconversion.....	29

1.8.2 <i>The Properties and Advantages of UCNPs</i>	31
1.9 SYNTHESIS OF LN-DOPED UCNPs	32
1.9.1 <i>Thermal Decomposition Method</i>	32
1.9.2 <i>Hydrothermal Synthesis Method</i>	33
1.9.3 <i>Ionothermal Synthesis Method</i>	34
1.10 CONCLUSION	35
2 LITERATURE REVIEW: SUPRAMOLECULAR INTERACTIONS INDUCED SURFACE MODIFICATION AND CONJUGATION OF UPCONVERSION NANOPARTICLES	36
2.1 INTRODUCTION.....	37
2.2 HYDROPHILIC MODIFICATION APPROACHES ON THE SURFACE OF UCNPs	37
2.2.1 <i>Overview</i>	37
2.2.2 <i>Ionic and Dipolar Interaction</i>	38
2.2.3 <i>Hydrophobic Effect</i>	44
2.2.4 <i>Organic Reactions on Original Ligand</i>	45
2.2.5 <i>Inorganic Coating</i>	46
2.3 SUPRAMOLECULAR INDUCED ORGANIC-INORGANIC SELF-ASSEMBLY OF UCNPs.	47
2.3.1 <i>Self-Assembly Based on Hydrophobic Effect</i>	47
2.3.2 <i>Self-Assembly Based on Ionic-Dipole Interaction</i>	49
2.3.3 <i>Self-Assembly Based on π Interaction</i>	49
2.4 SUPRAMOLECULAR INDUCED INORGANIC-INORGANIC SELF-ASSEMBLY OF UCNPs	50
2.4.1 <i>Inorganic-Inorganic Self-Assembly Based on Ion-Dipole Interaction</i>	50
2.4.2 <i>Inorganic-Inorganic Self-Assembly Based on Hydrophobic Effect</i>	51
2.4.3 <i>Inorganic-Inorganic Self-Assembly Based on Hydrogen Bond</i>	52
2.4.4 <i>Inorganic-Inorganic Self-Assembly Based on Inorganic Assistance</i>	53
2.4.5 <i>Inorganic-Inorganic Self-Assembly Based on Template Control</i>	53

3 THE SURFACE INVESTIGATION OF OLEIC ACID STABILIZED UPCONVERSION NANOPARTICLE.....	55
3.1 INTRODUCTION.....	56
3.2 EXPERIMENTAL SECTION.....	57
3.2.1 <i>Materials</i>	57
3.2.2 <i>Methods</i>	57
3.2.3 <i>Synthesis of Ln-UCNPs (NaYF₄: 20%Yb³⁺ / 2% Er³⁺)</i>	59
3.3 RESULTS AND DISCUSSION.....	60
3.3.1 <i>Characterisations of OA-UCNPs</i>	60
3.3.2 <i>Crystal Calculation</i>	64
3.3.3 <i>Calculation of Coverage of OA on the Surface of OA-UCNPs</i>	69
3.4 CONCLUSIONS.....	71
4 SELF-ASSEMBLY INDUCED MOLECULAR CONJUGATION OF CYCLODEXTRIN-STABILIZED UPCONVERSION NANOPARTICLES FOR INCREASING THE BIOCOMPATIBILITY OF ANTI-CANCER DRUG	72
4.1 INTRODUCTION.....	73
4.2 EXPERIMENTAL SECTION.....	76
4.2.1 <i>Materials</i>	76
4.2.2 <i>Methods</i>	77
4.2.3 <i>Synthesis and Preparation</i>	78
4.2.4 <i>Cytotoxicity of CD-UCNPs</i>	82
4.2.5 <i>Bioavailability of CD-UCNPs-DOX</i>	82
4.3 RESULTS AND DISCUSSION.....	82
4.3.1 <i>Structure Characterizations of CDs-COONa</i>	82
4.3.2 <i>Binding Behaviour of Organically Functional Groups</i>	90
4.3.3 <i>Morphology of CD-UCNPs</i>	93
4.3.4 <i>Surface modifications of UCNPs</i>	94

4.3.5 Drug Delivery Study.....	105
4.3.6 Drug Release Studies.	114
4.3.7 Cytotoxicity	116
4.3.8 Bioavailability of DOX.....	117
4.4 CONCLUSIONS	118
5 SELF-ASSEMBLY INDUCED PROTEIN CONJUGATION OF UPCONVERSION NANOPARTICLES FOR CELL TARGET IMAGING.....	120
5.1 INTRODUCTION.....	121
5.2 EXPERIMENTAL SECTION.....	122
5.2.1 Materials	122
5.2.2 Methods	123
5.2.3 Synthesis and Preparation	125
5.2.4 Cell Study.....	129
5.3 RESULTS AND DISCUSSION	130
5.3.1 Materials Characterizations	130
5.3.2 Binding Behaviours.....	139
5.3.3 <i>in vitro</i> Cell Study	152
5.4 CONCLUSIONS	155
6 SELF-ASSEMBLY INDUCED FÖRSTER RESONANCE ENERGY TRANSFER SYSTEM BASED ON UPCONVERSION NANOPARTICLES WITH GOLD NANOPARTICLES	156
6.1 INTRODUCTION.....	157
6.2 EXPERIMENTAL SECTION.....	158
6.2.1 Materials	158
6.2.2 Methods	160
6.2.3 Synthesis and Preparation	160
6.2.4 Self-Assembly and Competitive Binding	161

6.3 RESULTS AND DISCUSSION	162
6.3.1 <i>Design and Mechanism of FRET system</i>	162
6.3.2 <i>Binding Behaviour</i>	164
6.3.3 <i>Materials Characterization</i>	168
6.3.4 <i>Emission Study</i>	172
6.3.5 <i>Competitive Binding Study</i>	173
6.4 CONCLUSION	174
7 CONCLUSION	175
8 REFERENCES	178

LIST OF TABLES

TABLE 2-1. EXAMPLES OF LIGAND-EXCHANGE BASED ON ION-DIPOLE INTERACTIONS ON THE SURFACE OF UCNPs.	43
TABLE 2-2. EXAMPLES OF ORIGINAL LIGAND REACTION.	46
TABLE 2-3. EXAMPLES OF INORGANIC MODIFICATION ON THE UCNPs.	46
TABLE 3-1. ALL PREDICTED BINDING MODES OF OA ON THE SURFACE OF B-NAYF ₄	67
TABLE 3-2. SUMMARY OF BINDING MODES OF OA ON THE SURFACE OF THE B-NAYF ₄ CRYSTAL.	68
TABLE 4-1. THE COVERAGE OF CDs ON THE SURFACE OF UCNPs.	100
TABLE 4-2. THE SUMMARY OF BINDING CONSTANTS OF CD-UCNPs WITH DOX.	105
TABLE 4-3. WEIGHT LOSS OF CD-UCNPs BEFORE AND AFTER LOADING DOX AND THE LOADING EFFICIENCY.	114
TABLE 5-1. BINDING CONSTANTS OF AMINO ACIDS AND 1-ADAMANTANECARBOXYLIC ACID WITH CB[7].	144
TABLE 5-2. THE EMISSION STABILITY OF CB-UCNP@IGG-ADC.	150
TABLE 5-3. FREE IGG PERCENTAGE IN MEDIA.	151
TABLE 6-1. THE COMPLEX STABILITY CONSTANT (K_A) AND THERMODYNAMIC PARAMETERS FOR THE 1:1 INCLUSION COMPLEXATION OF CB[7] WITH L-PHE/AD IN PBS BUFFER (pH=7.4) AT 25 °C.	167

LIST OF FIGURES

FIGURE 1-1. THE DIFFERENCE BETWEEN (A). MOLECULAR (TRADITIONAL) CHEMISTRY AND (B). SUPRAMOLECULAR CHEMISTRY.	4
FIGURE 1-2. HOST-GUEST BASED SUPRAMOLECULAR SYSTEM FROM MOLECULAR BUILDING BLOCKS.	5
FIGURE 1-3. SELF-ASSEMBLED BASED SUPRAMOLECULAR SYSTEM FROM MOLECULAR BUILDING BLOCKS.	6
FIGURE 1-4. THE SUMMARY OF SUPRAMOLECULAR INTERACTIONS.....	6
FIGURE 1-5. EXAMPLES AND MECHANISMS OF ELECTROSTATIC INTERACTIONS: ION-ION INTERACTION (LEFT), ION-DIPOLE INTERACTION (MIDDLE), AND DIPOLE-DIPOLE INTERACTION (RIGHT).	7
FIGURE 1-6. THE TYPICAL BINDING BEHAVIOUR OF HYDROGEN BOND BETWEEN A CARBOXYL ACCEPTOR AND A SECONDARY AMINE DONOR (A) AND THE STANDARD BINDING MODE BETWEEN AN ACCEPTOR AND A DONOR IN A HYDROGEN BOND (B)....	8
FIGURE 1-7. TWO COMMON PRIMARY HYDROGEN BOND (BLACK DASHED LINE) MODES OF (A) ALL ACCEPTORS MOLECULE TO ALL DONOR MOLECULES (DDD AND AAA) AND (B) TWO MIXED DONOR/ACCEPTOR MOLECULES (DAD AND ADA). SECONDARY HYDROGEN INTERACTIONS (BLUE HASHED LINE) PROVIDING ATTRACTIONS BETWEEN ADJACENT GROUPS IN DDD AND AAA ARRAYS, AND THE REPULSIONS (RED TWO DIRECTION ANGLE) FROM DAD AND ADA ARRAYS.....	9
FIGURE 1-8. THE HYDROGEN BONDS BETWEEN BASE-PAIRS (GUANINE AND CYTOSINE) IN DNA.	10
FIGURE 1-9. TWO MAIN π - π INTERACTIONS: (A) FACE-TO-FACE INTERACTIONS, AND (B) EDGE-TO-FACE INTERACTIONS.	10

FIGURE 1-10. A VAN DER WAALS INTERACTION BETWEEN TWO ATOMS.....	11
FIGURE 1-11. AN EXAMPLE OF THE HYDROPHOBIC EFFECT.	12
FIGURE 1-12. THE INDUCED-FIT MODEL OF SUBSTRATE BINDING.	13
FIGURE 1-13. A MODEL OF ION SURROUNDED BY (A) SIX UNIDENTATE AMMONIA LIGANDS AND (B) THREE BIDENTATE ETHYLENEDIAMINE LIGANDS.	14
FIGURE 1-14. A MODEL OF PREORGANISATION OF HOST CONFORMATION.	15
FIGURE 1-15. THE PROCESS OF THE EFFECT OF SOLVENT MOLECULES ON THE FORMATION OF A HOST-GUEST SYSTEM.....	18
FIGURE 1-16. THE MOLECULAR STRUCTURES OF SEVERAL KINDS OF CROWN ETHERS: (A) 12- CROWN-4, (B) 15-CROWN-5, (C) 18-CROWN-6, (D) AZA-18-CROWN-6, AND (E) BENZO- 18-CROWN-6	19
FIGURE 1-17. THE COMPLEX OF 18-CROWN-6 WITH POTASSIUM.	20
FIGURE 1-18. THE STRUCTURES OF CDs (A) A-CD, (B) B-CD, AND (C) Γ -CD.	20
FIGURE 1-19. THE STRUCTURE OF CYCLOBIS(PARAQUAT-P-PHENYLENE) "BLUE BOX"....	21
FIGURE 1-20. THE STRUCTURE OF C[N]A.....	21
FIGURE 1-21. THE STRUCTURES OF CB[N].	22
FIGURE 1-22. THE STRUCTURES OF P[N]As.....	23
FIGURE 1-23. THE STRUCTURE OF BB[6] AND THE SYNTHETIC METHOD.	24
FIGURE 1-24. SCHEMATIC ILLUSTRATION OF SELF-ASSEMBLY.	25
FIGURE 1-25. SOME MODELS OF (A) ROTAXANE; (B) PSEUDOROTAXANE WITH ONE STOPPER; (C) PSEUDOROTAXANE WITHOUT STOPPERS AND (D) POLYROTAXANE.....	26
FIGURE 1-26. A MODEL OF TYPICAL CATENANE.....	27

FIGURE 1-27. SOME EXAMPLES OF SYNTHETIC MOLECULAR MACHINES: (A) MOLECULAR MOTOR, (B) MOLECULAR SWITCH, AND MOLECULAR SHUTTLE.	28
FIGURE 1-28. AN EXAMPLE OF BIOLOGICAL MOLECULAR MACHINES: RIBOSOME'S TRANSLATION.....	28
FIGURE 1-29. SCHEME OF ESA. AN ION OR ELECTRON AT THE GROUND STAGE ABSORBS TWO LOWER ENERGY PHOTONS AND EMITS A HIGHER ENERGY PHOTON WHEN JUMPING BACK TO THE GROUND STATE.	30
FIGURE 1-30. THE SCHEME OF PA.....	30
FIGURE 1-31. ENERGY TRANSFER PROCESSES BETWEEN TWO IONS: (A) RESONANT NON-RADIATIVE TRANSFER; (B) PHONON-ASSISTED NON-RADIATIVE TRANSFER. (S: SENSITIZER, A: ACTIVATOR).....	31
FIGURE 1-32. SCHEMATIC ILLUSTRATION OF THE GROWTH STAGES OF B-NAYF ₄ :YB,ER NANOCRYSTALS VIA A DELAYED NUCLEATION PATHWAY. RE: Y, YB, ER; OA: OLEIC ACID; OM: OLEYLAMINE. (MAI <i>ET AL.</i> , 2007).....	32
FIGURE 1-33. SCHEMATIC ILLUSTRATION OF THE GROWTH PROCESS OF A-NAYF ₄ :YB,ER NANOCRYSTALS FROM B-NAYF ₄ :YB,ER MONOMERS VIA A DELAYED A → B PHASE TRANSITION. (MAI <i>ET AL.</i> , 2007).....	33
FIGURE 1-34. NANO/MICROCRYSTALS OF UPCONVERSION MATERIALS BY HYDROTHERMAL SYNTHESIS. (CAO <i>ET AL.</i> 2011; FAN <i>ET AL.</i> 2006; LI <i>ET AL.</i> 2007; YI <i>ET AL.</i> 2002; ZHANG <i>ET AL.</i> 2007)	34
FIGURE 1-35. THE IONOTHERMAL SYNTHESIS OF HEXAGONAL-PHASE NAYF ₄ : YB ³⁺ , ER ³⁺ /TM ³⁺ : THE CHARACTERIZATION AND SPECTRA. (LIU <i>ET AL.</i> 2009)	35
FIGURE 2-1. THE OVERVIEW OF SURFACE MODIFICATION OF UCNPs BASED ON SURFACE BINDING MECHANISM.	38

FIGURE 2-2. THE LIGAND EXCHANGE REACTION OF OA-UCNP WITH PEG-PHOSPHATE. (BOYER ET AL. 2010)	40
FIGURE 2-3. THE TWO-STEP LIGAND-EXCHANGED METHOD ON THE SURFACE OF UCNPs BY USING ACID.	41
FIGURE 2-4. THE TWO-STEP LIGAND-EXCHANGED METHOD ON THE SURFACE OF UCNPs BY USING NOBF ₄ . (MUHR ET AL. 2014).....	41
FIGURE 2-5. THE LIGAND-EXCHANGED METHOD BY USING POLYMER. (HE ET AL. 2013)..	42
FIGURE 2-6. THE STRUCTURES OF OA AND CTAB.....	45
FIGURE 2-7. THE LIGAND-EXCHANGED METHOD BY USING HYDROPHOBIC EFFECT. (MUHR ET AL. 2014).....	45
FIGURE 2-8. AN EXAMPLE OF SURFACE CONJUGATION BY USING HYDROPHOBIC INTERACTIONS. (CEN ET AL. 2014).....	47
FIGURE 2-9. THE POLYMER ASSISTED SELF-ASSEMBLY BETWEEN UCNPs AND DOX. (ZHAO ET AL. 2017).....	48
FIGURE 2-10. THE HOST-GUEST (HYDROPHOBIC) INTERACTION INDUCED SELF-ASSEMBLY SYSTEM WITH GUEST MODIFIED UCNPs. (LIU ET AL. 2010).....	48
FIGURE 2-11. THE HOST-GUEST (HYDROPHOBIC) INTERACTION INDUCED SELF-ASSEMBLY SYSTEM WITH HOST MODIFIED UCNPs. (WANG ET AL. 2016).....	48
FIGURE 2-12. THE LAYER-BY-LAYER SYSTEM ON COATING ON THE SURFACE OF UCNPs AND THE pH CONTROLLED METHOD. (WANG <i>ET AL.</i> , 2013)	49
FIGURE 2-13. THE UCNP SENSOR BASED ON π - π INTERACTION. (WANG, WU & LIU 2013)	50
FIGURE 2-14. THE SELF-ASSEMBLY STRUCTURE OF UCNPs WITH G-C ₃ N ₄ BY ION-DIPOLE INTERACTION. (CHENG ET AL. 2015).....	51

FIGURE 2-15. THE SELF-ASSEMBLY SYSTEM BETWEEN PLNPs AND UCNPs BECAUSE OF HYDROPHOBIC EFFECT. (QIU ET AL. 2017)	51
FIGURE 2-16. THE SELF-ASSEMBLED ARCHITECTURES BETWEEN UCNPs AND AUNPs BY USING HYDROGEN BONDS. (SUN ET AL. 2016)	52
FIGURE 2-17. TRANSMISSION ELECTRON MICROSCOPY (TEM) IMAGES OF TiO ₂ COMPOSITES ASSISTED SELF-ASSEMBLY STRUCTURE BETWEEN Fe ₃ O ₄ NANOPARTICLES AND UCNPs. (LV ET AL. 2018).....	53
FIGURE 2-18. THE PROCESS OF TEMPLATE-ASSISTED SELF-ASSEMBLY BETWEEN UCNPs AND AUNPs. (GREYBUSH ET AL. 2014)	54
FIGURE 3-1. THE HEXAGONAL CRYSTAL OF B-NAYF ₄ -BASED UCNPs: (A) THE MODEL OF B-NAYF ₄ -BASED UCNPs; (B) THE {001} CRYSTAL FACET; (C) THE {100} CRYSTAL FACET.....	56
FIGURE 3-2. THE CRYSTAL UNIT OF HEXAGONAL B-NAYF ₄ -BASED UCNP. THE YELLOW DOTS STAND FOR SODIUM; THE GREEN DOTS STAND FOR YTTTRIUM. NOTE: THESE UNMARKED SMALL GREY DOTS ARE FLUORINE.	57
FIGURE 3-3. SCHEMATIC OF THE EXPERIMENTAL CONFIGURATION FOR MEASURING THE EMISSION OF UCNPs UNDER CONTINUOUS-WAVE 980 NM DIODE LASER.....	58
FIGURE 3-4. THE OPTICAL PROPERTIES OF THE OA-UCNPs (NAYF ₄ : 20% YB ³⁺ / 2% ER ²⁺): (A) THE EMISSION OF THE OA-UCNPs (NAYF ₄ : 20%YB ³⁺ / 2% ER ³⁺) AND (B) THE UPCONVERTING MECHANISM OF THE OA-UCNPs (NAYF ₄ : 20%YB ³⁺ / 2% ER ³⁺). ..	60
FIGURE 3-5. THE XRD PATTERNS OF THE OA-UCNPs (B-NAYF ₄ : 2%ER ³⁺ / 20%YB ³⁺ @ OA).....	61
FIGURE 3-6. THE ¹ H NMR SPECTRA (500 MHZ) OF (A) FREE OA MOLECULES AND (B) OA-UCNPs (NAYF ₄ : 20%YB ³⁺ /2%ER ³⁺ @OA) IN CDCL ₃ -D AT 25 °C.	62
FIGURE 3-7. FT-IR SPECTRA OF OA (RED) AND OA-UCNPs (BLUE).	62

FIGURE 3-8. XPS SPECTRUM (A) O1s AND (B) C1s OF OA-UCNP.....	63
FIGURE 3-9. THE TGA AND DTGA CURVES: (A) THE TGA (RED) AND DTGA (BLUE) OF OA MOLECULE, AND (B) THE TGA OF OA-UCNPs.	64
FIGURE 3-10. B-NaYF ₄ NANOCRYSTAL UNITS: THE DISTANCE BETWEEN TWO ADJUST Y ³⁺ ATOMS IS 5.96 Å IN {001} FACET (LEFT); THE TWO TYPES OF DISTANCES BETWEEN TWO ADJUST Y ³⁺ ATOMS ARE 5.96 Å AND 3.53 Å/3.69 Å (RIGHT).....	64
FIGURE 3-11. THE STRUCTURE OF OA. (A). THE STRUCTURE OF OA; (B). THE RESONANCE STRUCTURE OF OA; (C). THE STRUCTURE OF OLEATE HYBRID.	65
FIGURE 3-12. CRYSTALLOGRAPHIC ANALYSIS OF BOTH OA-UCNPs: THE SIDE VIEW (A) AND TOP VIEW (C) OF {001} IN OA-UCNPs; THE SIDE VIEW (B) AND TOP VIEW (D) OF {100} IN OA-UCNPs.	68
FIGURE 3-13. THE MODEL OF A HEXAGONAL UCNP.	69
FIGURE 4-1. THE STRUCTURES OF FUNCTIONAL CDs MENTIONED IN THIS CHAPTER: (A) A-CD-COONa, (B) B-CD-COONa, (C) Γ -CD-COONa, (D) B-CD-SO ₃ Na, AND (E) B-CD-PO ₃ Na ₂	75
FIGURE 4-2. (A) THE MECHANISM OF THE SURFACE MODIFICATION OF CD-UCNPs AND MOLECULAR CONJUGATION WITH HOST-GUEST INTERACTIONS. (B) THE TWO SIDE VIEWS OF THE CONJUGATION STRUCTURE.	76
FIGURE 4-3. THE SYNTHESIS OF A-CD-COONa.....	79
FIGURE 4-4. THE SYNTHESIS OF B-CD-COONa.....	80
FIGURE 4-5. THE SYNTHESIS OF Γ -CD-COONa.	80
FIGURE 4-6. THE BASIC STRUCTURE OF CDs AND THE NUMBERS OF PROTONS. (R = H OR CARBOXYLATE).....	83
FIGURE 4-7. ¹ H NMR SPECTRUM OF A-CD-COONa IN D ₂ O AT 25 °C (500 MHz).	83

FIGURE 4-8. ^{13}C NMR SPECTRUM OF A-CD-COONa IN D_2O AT 25 °C (125 MHz).	84
FIGURE 4-9. ^1H NMR SPECTRUM OF B-CD-COONa IN D_2O AT 25 °C (500 MHz).	84
FIGURE 4-10. ^{13}C NMR SPECTRUM OF B-CD-COONa IN D_2O AT 25 °C (125 MHz).	85
FIGURE 4-11. ^1H NMR SPECTRUM OF Γ -CD-COONa IN D_2O AT 25 °C (500 MHz).	85
FIGURE 4-12. ^{13}C NMR SPECTRUM OF Γ -CD-COONa IN D_2O AT 25 °C (125 MHz).	86
FIGURE 4-13. RAMAN SPECTRA: (A). A-CD (BLACK) AND A-CD-COONa (RED); (B). B-CD (BLACK) AND B-CD-COONa (RED); (C). Γ -CD (BLACK) AND Γ -CD-COONa (RED).	87
FIGURE 4-14. FT-IR SPECTRA: (A). A-CD (BLACK) AND A-CD-COONa (RED); (B). B-CD (BLACK) AND B-CD-COONa (RED); (C). Γ -CD (BLACK) AND Γ -CD-COONa (RED).	88
FIGURE 4-15. TGA AND DTGA CURVES OF (A) A-CD, (B) B-CD, (C) Γ -CD, (D) A-CD-COONa, (E) B-CD-COONa, AND (F) Γ -CD-COONa.....	89
FIGURE 4-16. THE FT-IR SPECTRA OF FREE SDS (BLUE), SDS-UCNPs (RED), AND OA-UCNPs (BLACK).	91
FIGURE 4-17. THE BINDING PREDICTION OF SULPHATE WITH Y ATOM FROM UCNP SURFACE.	91
FIGURE 4-18. THE FT-IR SPECTRA OF FREE SDP (BLUE), SDP-UCNPs (RED), AND OA-UCNPs (BLACK).	92
FIGURE 4-19. THE BINDING PREDICTION OF SDP WITH Y ATOM FROM UCNP SURFACE. .	93
FIGURE 4-20. TEM IMAGES OF (A) A-CD-COONa-UCNP, (B) B-CD-COONa-UCNP, (C) Γ -CD-COONa-UCNP, (D) B-CD-SO ₃ Na-UCNP, (E) B-CD-PO ₃ Na ₂ -UCNP AND (F)OA-UCNP.....	93

FIGURE 4-21. PARTICLE SIZES (DLS) OF A-CD-COONa-UCNP (IN WATER), B-CD-COONa-UCNP (IN WATER), Γ -CD-COONa-UCNP (IN WATER), B-CD-SO ₃ Na-UCNP (IN WATER), B-CD-PO ₃ Na ₂ -UCNP (IN WATER), A-CD-COONa-UCNP-DOX (IN WATER), B-CD-COONa-UCNP-DOX (IN WATER), Γ -CD-COONa-UCNP-DOX (IN WATER), B-CD-SO ₃ Na-UCNP-DOX (IN WATER), B-CD-PO ₃ Na ₂ -UCNP-DOX (IN WATER), AND OA-UCNP (IN CYCLOHEXANE).	94
FIGURE 4-22. RAMAN SPECTRA OF CDS-COONa (RED) AND CD-COONa-UCNPs (BLUE). (A, B) A-CD-COONa AND A-CD-COONa-UCNP, (C, D) B-CD-COONa AND B-CD-COONa-UCNP, (E, F) Γ -CD-COONa AND Γ -CD-COONa-UCNP.....	95
FIGURE 4-23. RAMAN SPECTRA OF (A, B) B-CD-SO ₃ Na (RED) AND B-CD-SO ₃ Na-UCNP (BLUE), (C, D) B-CD-PO ₃ Na ₂ (RED) AND B-CD-PO ₃ Na ₂ -UCNP (BLUE).....	96
FIGURE 4-24. FT-IR SPECTRA OF (A) A-CD-COONa (RED) AND A-CD-COONa-UCNP (BLUE), (B) B-CD-COONa (RED) AND B-CD-COONa-UCNP (BLUE), (C) Γ -CD-COONa (RED) AND Γ -CD-COONa-UCNP (BLUE).	97
FIGURE 4-25. FT-IR SPECTRA OF (A) B-CD-SO ₃ Na (RED) AND B-CD-SO ₃ Na-UCNP (BLUE), (B) B-CD-PO ₃ Na ₂ (RED) AND B-CD-PO ₃ Na ₂ -UCNP (BLUE).....	98
FIGURE 4-26. TGA CURVES OF (A) A-CD-COONa (RED) AND A-CD-COONa-UCNP (BLUE), (B) B-CD-COONa (RED) AND B-CD-COONa-UCNP (BLUE), (C) Γ -CD-COONa (RED) AND Γ -CD-COONa-UCNP (BLUE).	99
FIGURE 4-27. TGA CURVES OF (A) B-CD-SO ₃ Na (RED) AND B-CD-SO ₃ Na-UCNP (BLUE), (B) B-CD-PO ₃ Na ₂ (RED) AND B-CD-PO ₃ Na ₂ -UCNP (BLUE).....	100
FIGURE 4-28. ITC MEASUREMENTS: (A). THE COMPLEXATION REACTION OF B-CD-COONa (1 mM) WITH DOX (0.5 MMOL/L) FOR EACH INJECTION DURING A CALORIMETRIC TITRATION AT 25 °C. TOP: RAW ITC DATA FOR 25 SEQUENTIAL INJECTIONS (2 μ L PER INJECTION) OF B-CD-COONa SOLUTION (1 MMOL/L) INTO DOX SOLUTION (0.5	

MMOL/L). BOTTOM: NET HEAT EFFECTS OBTAINED BY SUBTRACTING THE DILUTION HEAT FROM THE REACTION HEAT, FITTED BY “INDEPENDENCE” MODEL. (B) THE DILUTION HEAT OF B-CD-COONa IN H₂O AT 25 °C. TOP: RAW ITC DATA FOR 25 SEQUENTIAL INJECTIONS (2 μL PER INJECTION) OF B-CD-COONa SOLUTION (1 MMOL/L) INTO H₂O. BOTTOM: HEAT EFFECTS OF THE DILUTION WITH B-CD-COONa (1 MMOL/L) FOR EACH INJECTION DURING A CALORIMETRIC TITRATION AT 25 °C. 101

FIGURE 4-29. ITC MEASUREMENTS: (A). THE COMPLEXATION REACTION OF Γ -CD-COONa (1 mM) WITH DOX (0.5 MMOL/L) FOR EACH INJECTION DURING A CALORIMETRIC TITRATION AT 25 °C. TOP: RAW ITC DATA FOR 25 SEQUENTIAL INJECTIONS (2 μL PER INJECTION) OF Γ -CD-COONa SOLUTION (1 MMOL/L) INTO DOX SOLUTION (0.5 MMOL/L). BOTTOM: NET HEAT EFFECTS OBTAINED BY SUBTRACTING THE DILUTION HEAT FROM THE REACTION HEAT, FITTED BY “INDEPENDENCE” MODEL. (B) THE DILUTION HEAT OF Γ -CD-COONa IN H₂O AT 25 °C. TOP: RAW ITC DATA FOR 25 SEQUENTIAL INJECTIONS (2 μL PER INJECTION) OF Γ -CD-COONa SOLUTION (1 MMOL/L) INTO H₂O. BOTTOM: HEAT EFFECTS OF THE DILUTION WITH Γ -CD-COONa (1 MMOL/L) FOR EACH INJECTION DURING A CALORIMETRIC TITRATION AT 25 °C. 102

FIGURE 4-30. ITC MEASUREMENTS: (A). THE COMPLEXATION REACTION OF B-CD-SO₃Na (1 mM) WITH DOX (0.5 MMOL/L) FOR EACH INJECTION DURING A CALORIMETRIC TITRATION AT 25 °C. TOP: RAW ITC DATA FOR 25 SEQUENTIAL INJECTION (2 μL PER INJECTION) OF B-CD-SO₃Na SOLUTION (1 MMOL/L) INTO DOX SOLUTION (0.5 MMOL/L). BOTTOM: NET HEAT EFFECTS OBTAINED BY SUBTRACTING THE DILUTION HEAT FROM THE REACTION HEAT, FITTED BY “INDEPENDENCE” MODEL. (B) THE DILUTION HEAT OF B-CD-SO₃Na IN H₂O AT 25 °C. TOP: RAW ITC DATA FOR 25 SEQUENTIAL INJECTIONS (2 μL PER INJECTION) OF B-CD-SO₃Na SOLUTION (1 MMOL/L) INTO H₂O. BOTTOM: HEAT EFFECTS OF THE DILUTION WITH B-CD-SO₃Na (1 MMOL/L) FOR EACH INJECTION DURING A CALORIMETRIC TITRATION AT 25 °C. 103

FIGURE 4-31. ITC MEASUREMENTS: (A). THE COMPLEXATION REACTION OF B-CD-PO₃NA₂ (1 mM) WITH DOX (0.5 MMOL/L) FOR EACH INJECTION DURING A CALORIMETRIC TITRATION AT 25 °C. TOP: RAW ITC DATA FOR 25 SEQUENTIAL INJECTION (2 μL PER INJECTION) OF B-CD-PO₃NA₂ SOLUTION (1 MMOL/L) INTO DOX SOLUTION (0.5 MMOL/L). BOTTOM: NET HEAT EFFECTS OBTAINED BY SUBTRACTING THE DILUTION HEAT FROM THE REACTION HEAT, FITTED BY “INDEPENDENCE” MODEL. (B) THE DILUTION HEAT OF B-CD-PO₃NA₂ IN H₂O AT 25 °C. TOP: RAW ITC DATA FOR 25 SEQUENTIAL INJECTIONS (2 μL PER INJECTION) OF B-CD-PO₃NA₂ SOLUTION (1 MMOL/L) INTO H₂O. BOTTOM: HEAT EFFECTS OF THE DILUTION WITH B-CD-PO₃NA₂ (1 MMOL/L) FOR EACH INJECTION DURING A CALORIMETRIC TITRATION AT 25 °C. 104

FIGURE 4-32. RAMAN SPECTRA OF (A) A-CD-COONa-UCNP AND A-CD-COONa-UCNP-DOX, (B) B-CD-COONa-UCNP AND B-CD-COONa-UCNP-DOX, (C) Γ-CD-COONa-UCNP AND Γ-CD-COONa-UCNP-DOX. 106

FIGURE 4-33. RAMAN SPECTRA OF (A,B) B-CD-SO₃Na-UCNP AND B-CD-SO₃Na-UCNP-DOX, (C,D) B-CD-PO₃NA₂-UCNP AND B-CD-PO₃NA₂-UCNP-DOX. 107

FIGURE 4-34. FT-IR SPECTRA OF (A) A-CD-COONa-UCNP AND A-CD-COONa-UCNP-DOX, (B) B-CD-COONa-UCNP AND B-CD-COONa-UCNP-DOX, (C) Γ-CD-COONa-UCNP AND Γ-CD-COONa-UCNP-DOX, (D) B-CD-SO₃Na-UCNP AND B-CD-SO₃Na-UCNP-DOX, (E) B-CD-PO₃NA₂-UCNP AND B-CD-PO₃NA₂-UCNP-DOX, AND (F) DOX. 108

FIGURE 4-35. UV-VIS SPECTRA OF (A) A-CD-COONa-UCNP-DOX, (B) B-CD-COONa-UCNP-DOX, (C) Γ-CD-COONa-UCNP-DOX, (D) B-CD-SO₃Na-UCNP-DOX, AND (E) B-CD-PO₃NA₂-UCNP-DOX. 109

FIGURE 4-36. EMISSION SPECTRA OF (A) A-CD-COONa-UCNP, (B) A-CD-COONa-UCNP-DOX, (C) B-CD-COONa-UCNP, (D) B-CD-COONa-UCNP-DOX, (E) Γ-CD-COONa-UCNP, AND (F) Γ-CD-COONa-UCNP-DOX. 110

FIGURE 4-37. EMISSION SPECTRA OF (A) B-CD-SO ₃ NA-UCNP, (B) B-CD-SO ₃ NA-UCNP-DOX, (C) B-CD-PO ₃ NA ₂ -UCNP, AND (D) B-CD-PO ₃ NA ₂ -UCNP-DOX.....	111
FIGURE 4-38. TGA CURVES OF (A) A-CD-COONa-UCNP AND A-CD-COONa-UCNP-DOX, (B) B-CD-COONa-UCNP AND B-CD-COONa-UCNP-DOX, AND (C) Γ -CD-COONa-UCNP AND Γ -CD-COONa-UCNP-DOX.....	112
FIGURE 4-39. TGA CURVES OF (A) B-CD-SO ₃ NA-UCNP AND B-CD-SO ₃ NA-UCNP-DOX, AND (B) B-CD-PO ₃ NA ₂ -UCNP AND B-CD-PO ₃ NA ₂ -UCNP-DOX.	113
FIGURE 4-40. RELEASE PROFILES OF DOX FROM (A) A-CD-COONa-UCNP-DOX, (B) B-CD-COONa-UCNP-DOX, AND (C) Γ -CD-COONa-UCNP-DOX. THE DOX CONCENTRATION IN THE SOLUTION IS CARRIED OUT BY UV-VIS SPECTRA AND MONITORED VIA NANO DROP 2000. THE DETECTION WAVELENGTH IS 498 NM.....	115
FIGURE 4-41. RELEASE PROFILES OF DOX FROM (A) B-CD-SO ₃ NA-UCNP-DOX, AND (B) B-CD-PO ₃ NA ₂ -UCNP-DOX. THE DOX CONCENTRATIONS IN THE SOLUTIONS OF THESE SAMPLES ARE MONITORED BY UV-VIS SPECTRA <i>VIA</i> NANO DROP 2000. THE DETECTION WAVELENGTH IS 498 NM.....	116
FIGURE 4-42. <i>IN VITRO</i> CELL-GROWTH INHIBITION ASSAY FOR L929 CELL LINE (A) AND HALA CELL LINE (B) OBTAINED BY ADDING A-CD-COONa-UCNP (BLACK), B-CD-COONa-UCNP (RED), Γ -CD-COONa-UCNP (BLUE), B-CD-SO ₃ NA-UCNP (PINK), AND B-CD-PO ₄ NA ₂ -UCNP (GREEN).....	117
FIGURE 4-43. <i>IN VITRO</i> CELL-GROWTH INHIBITION ASSAY FOR L929 CELL LINE (A) AND HE LA CELL LINE (B) OBTAINED BY ADDING Γ -CD-COONa-UCNP-DOX (BLACK), B-CD-SO ₃ NA-UCNP-DOX (RED), B-CD-PO ₄ NA ₂ -UCNP-DOX (BLUE) AND DOX (PINK).....	118
FIGURE 5-1. CB[7]-BASED ONE-STEP HYDROPHILIC LIGAND EXCHANGE APPROACH WITHOUT REACTION CONJUGATION BY HOST-GUEST SELF-ASSEMBLY.....	122

FIGURE 5-2. PURIFICATION OF CB[7].	123
FIGURE 5-3. SYNTHESIS OF SA.	126
FIGURE 5-4. ¹ H NMR SPECTRUM OF SA IN D ₂ O AT 25°C (500 MHz).	126
FIGURE 5-5. ¹³ C NMR SPECTRUM OF SA IN D ₂ O AT 25°C (125 MHz).	127
FIGURE 5-6. FT-IT SPECTRUM OF SA.	127
FIGURE 5-7. SYNTHESIS OF 1-ADAMANTANECARBOXYLATE-MODIFIED IGG.	128
FIGURE 5-8. TGA CURVE OF CB-UCNP WITH DIFFERENT CONCENTRATIONS OF CB[7], 2 MM (RED), 5 MM (ORANGE), 10 MM (BLUE), COMPARED WITH OA-UCNP (BLACK).	131
FIGURE 5-9. DTGA CURVES OF FREE CB[7] AND CB-UCNPs WITH DIFFERENT CONCENTRATIONS OF CB[7], 2 MM (RED), 5 MM (ORANGE), 10 MM (BLUE).	132
FIGURE 5-10. THE TEM IMAGE OF (A) OA-UCNPs AND (B) CB-UCNPs. THE SIZE DISTRIBUTION OF (C) OA-UCNPs AND (D) CB-UCNPs.	133
FIGURE 5-11. THE SIZE OF OA-UCNPs IN CYCLOHEXANE (A) AND CB-UCNPs IN WATER (B).	134
FIGURE 5-12. THE XRD PATTERN OF CB-UCNPs (B-NaYF ₄ : 2%Er ³⁺ /20%Yb ³⁺ @CB[7]).	134
FIGURE 5-13. XPS SPECTRA OF OA-UCNPs (BLUE) AND CB-UCNPs (GREEN, 2 MM).	135
FIGURE 5-14. XPS SPECTRUM (O1s) OF CB-UCNPs.	136
FIGURE 5-15. XPS SPECTRUM (C1s) OF CB-UCNPs.	136
FIGURE 5-16. XPS SPECTRUM (N1s) OF CB-UCNP.	137
FIGURE 5-17. THE EMISSION SPECTRUM OF CB[7]-FUNCTIONAL NaYF ₄ NANOCRYSTAL CO- DOPED WITH 20% YB AND 2% ER (CB-UCNPs).	137

FIGURE 5-18. ^1H NMR SPECTRUM OF CB-UCNPs IN D_2O AT $25\text{ }^\circ\text{C}$	138
FIGURE 5-19. FT-IR SPECTRA: FREE OA (RED), OA-UCNP (BLUE), FREE CB[7] (ORANGE) AND CB-UCNPs (GREEN, 2 MM).	139
FIGURE 5-20. THE STRUCTURE OF CB[7].	140
FIGURE 5-21. THE BINDING MECHANISM OF CB[7] ON THE SURFACE OF NaYF_4	140
FIGURE 5-22. CRYSTALLOGRAPHIC ANALYSIS OF CB-UCNPs: THE SIDE VIEW (E) AND TOP VIEW (G) OF $\{001\}$ IN CB-UCNPs; THE SIDE VIEW (F) AND TOP VIEW (H) OF $\{100\}$ IN CB-UCNPs.	141
FIGURE 5-23. COMPARISON OF VISIBLE EMISSION BETWEEN THE CYCLOHEXANE LAYER BEFORE (A) AND AFTER (B) LIGAND EXCHANGE WITH CB[7] SOLUTION UNDER 980 NM LASER.	142
FIGURE 5-24. THE EMISSION SPECTRA OF CYCLOHEXANE LAYER: BEFORE EXCHANGE (GREEN) AND AFTER THE EXCHANGE (BLACK) UNDER 980 NM LASER.	143
FIGURE 5-25. BINDING CONTRASTS OF AMINO ACIDS AND 1-ADMANTANECARBOXYLIC ACID WITH CB[7].	144
FIGURE 5-26. BINDING MODEL OF SELF-ASSEMBLY.	146
FIGURE 5-27. CONJUGATION AMOUNT OF FUNCTIONAL GROUPS ON THE SURFACE OF CB- UCNPs AND OA-UCNPs.	147
FIGURE 5-28. CONJUGATION AVAILABILITY OF FUNCTIONAL GROUPS ON THE SURFACE OF CB-UCNPs AND OA-UCNPs.	149
FIGURE 5-29. BINDING RATE OF IGG-ADC ON THE SURFACE OF CB-UCNPs AND OA- UCNPs.	149
FIGURE 5-30. THE EMISSION STABILITY OF CB-UCNP@IGG-ADC.	151
FIGURE 5-31. FREE IGG PERCENTAGE IN MEDIA.	152

FIGURE 5-32. <i>IN VITRO</i> CELL-GROWTH INHIBITION ASSAY FOR HELA CANCER CELL LINE OBTAINED BY ADDING DIFFERENT CONCENTRATIONS OF CB-UCNPs.	153
FIGURE 5-33. CELL IMAGING OF CB-UCNP@IGG-ADC TARGETING ON THE SURFACE OF HELA CELLS. PHALLOIDIN-FITC STAINS THE FRAMEWORK OF THE CELL, DAPI STAINS NUCLEUS, WE PSEUDO BLUE COLOUR TO YELLOW FOR EASIER VISUALIZATION.	154
FIGURE 5-34. THE CELL IMAGING OF CB-UCNP@IGG-ADC ATTACHED ON THE SURFACE OF HELA CELL.....	154
FIGURE 6-1. THE PROCESS AND MECHANISM OF THE CONTROLLABLE FRET SYSTEM. I. ADDING THE L-PHE-AUNPs AND MIXING WITH CB-UCNPs; II. CB-UCNP AND L-PHE-AUNP FORM A FRET PAIR WITH SUPRAMOLECULAR HOST-GUEST INTERACTION. AUNPs QUENCH THE EMISSION OF UCNPs BECAUSE THE DISTANCE BETWEEN THE TWO TYPES OF NANOPARTICLES IS AROUND 1 NM; III. COMPETITIVE BINDING STEP: A KIND OF HIGHER BINDING GUEST MOLECULES (COMPARED WITH L-PHE, SUCH AS AD AND DERIVATIVES) CAN REPLACE AND OCCUPY THE CAVITIES OF CB[7] ON THE SURFACE OF UCNPs DUE TO THE COMPETITIVE BINDING; (IV). AFTER HIGHER BINDING MOLECULES (AD AND DERIVATIVES) FORM THE COMPLEX WITH CB[7] FROM THE SURFACE OF CB-UCNPs, L-PHE-AUNPs ARE GETTING FREE AGAIN. THE DISTANCE BETWEEN A CB-UCNP AND AN L-PHE-AUNP IS LARGER THAN 5 NM, AND THE EMISSION OF CB-UCNPs IS RECOVERED.....	159
FIGURE 6-2. THE SYNTHESIS OF THE DETECTION SYSTEM: I. THE SYNTHESIS OF OA-UCNPs; II. THE PREPARATION OF CB-UCNPs BY LIGAND-EXCHANGE; III. THE SYNTHESIS OF L-PHE-AUNPs; IV. SELF-ASSEMBLY FOR FORMING THE DETECTION SYSTEM.	162
FIGURE 6-3. THE MECHANISM OF FRET BETWEEN CB-UCNPs AND L-PHE-AUNPs.....	163
FIGURE 6-4. THE CALCULATION OF THE SIZE OF THE COMPLEXES: A. THE COMPLEX OF CB[7] AND L-PHE; B. THE COMPLEX OF CB[7] AND AD.	164

FIGURE 6-5. ITC MEASUREMENTS (A). THE COMPLEXATION REACTION OF CB[7] (2 MMOL/L) WITH L-PHE (20 MMOL/L) FOR EACH INJECTION DURING A CALORIMETRIC TITRATION AT 25 °C. TOP: RAW ITC DATA FOR 50 SEQUENTIAL INJECTIONS (1 μL PER INJECTION) OF L-PHE SOLUTION (20 MMOL/L) INTO CB[7] SOLUTION (2 MMOL/L). BOTTOM: NET HEAT EFFECTS OBTAINED BY SUBTRACTING THE DILUTION HEAT FROM THE REACTION HEAT, FITTED BY “INDEPENDENCE” MODEL. (B). THE COMPLEXATION REACTION OF CB[7] (2 MMOL/L) WITH AD (10 MMOL/L) FOR EACH INJECTION DURING A CALORIMETRIC TITRATION AT 25 °C. TOP: RAW ITC DATA FOR 50 SEQUENTIAL INJECTIONS (1 μL PER INJECTION) OF AD SOLUTION (10 MMOL/L) INTO CB[7] SOLUTION (2 MMOL/L). BOTTOM: NET HEAT EFFECTS OBTAINED BY SUBTRACTING THE DILUTION HEAT FROM THE REACTION HEAT, FITTED BY “INDEPENDENCE” MODEL. THE K_D OF THE COMPLEXATION OF CB[7] WITH L-PHE IS 5.588×10^{-5} M, THE ONE OF CB[7] WITH AD IS 4.377×10^{-7} M..... 165

FIGURE 6-6. THE DILUTION HEAT OF L-PHE IN PBS BUFFER (pH = 7.4) AT 25 °C. TOP: RAW ITC DATA FOR 50 SEQUENTIAL INJECTIONS (1 μL PER INJECTION) OF L-PHE SOLUTION (20 MMOL/L) INTO PBS BUFFER (pH=7.4). BOTTOM: HEAT EFFECTS OF THE DILUTION WITH L-PHE (20 MMOL/L) FOR EACH INJECTION DURING A CALORIMETRIC TITRATION AT 25 °C. THE DILUTION HEAT OF AD IN PBS BUFFER (pH = 7.4) AT 25 °C. TOP: RAW ITC DATA FOR 50 SEQUENTIAL INJECTIONS (1 μL PER INJECTION) OF AD SOLUTION (10 MMOL/L) INTO PBS BUFFER (pH=7.4). BOTTOM: HEAT EFFECTS OF THE DILUTION WITH AD (10 MMOL/L) FOR EACH INJECTION DURING A CALORIMETRIC TITRATION AT 25 °C..... 166

FIGURE 6-7. TWO TYPES OF COMPETITIVE BINDING MODES: (A) INHIBITION AND (B) REPLACEMENT..... 168

FIGURE 6-8. TEM IMAGES OF (A) CB-UCNPs AND (B) L-PHE-AUNPs. 169

FIGURE 6-9. THE SIZE DISTRIBUTIONS OF (A) CB-UCNPs AND (B) L-PHE-AUNPs. 169

FIGURE 6-10. THE HYDRATION SIZE OF (A) CB-UCNPs, (B) L-PHE-AUNPs, AND (3) SELF-ASSEMBLY OF CB-UCNPs AND L-PHE-AUNPs.....	169
FIGURE 6-11. THE STRUCTURE CHARACTERIZATIONS. FT-IR SPECTRA: A) <i>I.</i> L-PHE MOLECULES; <i>II.</i> L-PHE-AUNPs; B) <i>I.</i> CB[7] MOLECULES; <i>II.</i> CB-UCNPs; C) <i>I.</i> 1-AMINOADAMANTANE HYDROCHLORIDE (AD-NH ₃ CL); <i>II.</i> CB-UCNP SELF-ASSEMBLED WITH L-PHE-AUNPs (UCNP-CB-L-PHE-AUNPs); <i>III.</i> ADDING AD-NH ₃ CL INTO THE SELF-ASSEMBLED SYSTEM (UCNP-CB-AD & L-PHE-AUNPs). D) RAMAN SPECTRA: <i>I.</i> L-PHE-AUNPs; <i>II.</i> CB-UCNP SELF-ASSEMBLED WITH L-PHE-AUNPs (UCNP-CB-L-PHE-AUNPs); <i>III.</i> ADDING AD-NH ₃ CL INTO THE SELF-ASSEMBLED SYSTEM (UCNP-CB-AD & L-PHE-AUNPs).....	171
FIGURE 6-12. THE QUENCHING EXPERIMENT BETWEEN AUNPs WITH UCNPs. (A). EMISSION SPECTRA OF UCNPs BINDING WITH DIFFERENT CONCENTRATIONS OF AUNPs; (B). THE CURVE OF THE QUENCHING RATIO OF UCNPs WITH VARYING CONCENTRATIONS OF AUNPs.	173
FIGURE 6-13. THE EMISSION RECOVERY OF UCNPs WITH ADDING AD MOLECULES: THE EMISSION FOR 1 H MIXED (RED) AND 12 H MIXED (BLUE). MOLE RATIO IS AUNPs /UCNPs.	174

LIST OF ABBREVIATIONS AND ACRONYMS

3D: Three Dimensional

Ad: Amantadine Hydrochloride

ATR: Attenuated Total Reflectance

AuNP: Gold Nanoparticle

BB[n]: Bambus[n]uril

BSA: Bovine Serum Albumin

C[n]A: Calix[n]arene

CB[7]: Cucurbit[7]uril

CB[n]: Cucurbit[n]uril

CB-UCNP: Cucurbit[7]uril Stabilized Upconversion Nanoparticle

CB-UCNP@IgG-ADC: N-1-Adamantanecarboxyl Immunoglobulin G Self-Assembled
on the Surface of Cucurbit[7]uril Stabilized Upconversion Nanoparticle

CD: Cyclodextrin

CD-UCNP: Cyclodextrin Stabilized Upconversion Nanoparticle

CD-UCNPs-DOX: Doxorubicin Loaded Cyclodextrin Stabilized Upconversion
Nanoparticle

CTAB: Cetyltrimethylammonium Bromide

DAPI: 2-(4-Amidinophenyl)-6-Indolecarbamide Dihydrochloride

DLS: Dynamic Light Scattering

DMEM: Dulbecco's Modified Eagle's Medium

DMSO: Methyl Sulfoxide

DOX: Doxorubicin Hydrochlorate

DTGA: Differential Thermogravimetric Analysis

EDC: N-(3-Dimethylaminopropyl)-N'-Ethylcarbodiimide Hydrochloride

ErCl₃·6H₂O: Erbium (III) Chloride Hexahydrate

ESA: Excited State Absorption

EtOH: Ethanol

ETU: Energy Transfer Upconversion

FBS: Fetal Bovine Serum

FRET: Förster Resonance Energy Transfer

FT-IR: Fourier-Transform Infrared

HAuCl₄: Chloroauric Acid

IgG: Immunoglobulin G

IgG-ADC: N-1-Adamantanecarboxyl-IgG

ITC: Isothermal Titration Calorimetry

Ln: Lanthanide

Ln-UCNC: Lanthanide Doped Upconversion Nanocrystal

Ln-UCNP: Lanthanide Doped Upconversion Nanoparticle

L-Phe: L-Phenylalanine

L-Phe-AuNP: L-Phenylalanine Reduced Gold Nanoparticle

NH₄F: Ammonium Fluoride

MIM: Mechanically Interlocked Molecules

MTT: Thiazolyl Blue Tetrazolium Bromide

NMR: Nuclear Magnetic Resonance

NOBF₄: Nitrosyl Tetrafluoroborate

OA: Oleic Acid

OA-UCNP: Oleic Acid Stabilized Upconversion Nanoparticle

ODE: 1-Octadecene

OM: Oleylamine

PA: Photon Avalanche

P[n]A: Pillar[n]arene

PAH: Poly(Allylamine Hydrochloride)

PEG: Poly(Ethylene Glycol)

Phalloidin-FITC: Phalloidin-Fluorescein Isothiocyanate Labelled

PLNP: Persistent Luminescence Nanoparticle

PMPD: Poly(m-Phenylenediamine)

QD: Quantum Dots

SA: Sodium 1-Adamantanecarboxylate

SDP: Sodium Dodecyl Phosphate

SDS: Sodium Dodecyl Sulphate

TEM: Transmission Electron Microscopy

TGA: Thermogravimetric Analysis

THF: Tetrahydrofuran

UCNP: Upconversion Nanoparticle

UCNP-COOH: Direct Carboxyl-Modified Upconversion Nanoparticle

UV-vis: Ultraviolet Visible

XPS: X-Ray Photoelectron Spectra

XRD: X-Ray Diffraction

YbCl₃·6H₂O: Ytterbium (III) Chloride Hexahydrate

YCl₃·6H₂O: Yttrium (III) Chloride Hexahydrate

α-CD: α-Cyclodextrin

α-CD-COONa: Carboxylic α-Cyclodextrin Sodium Salt

α-CD-COOH-UCNP-DOX: Doxorubicin Loaded Carboxylic α-Cyclodextrin Stabilized
Upconversion Nanoparticle

β-CD: β-Cyclodextrin

β-CD-COOH: Carboxylic β-Cyclodextrin

β-CD-COONa: Carboxylic β-Cyclodextrin Sodium Salt

β-CD-COOH-UCNP-DOX: Doxorubicin Loaded Carboxylic β-Cyclodextrin Stabilized
Upconversion Nanoparticle

β-CD-PO₃Na₂: Phosphoric β-Cyclodextrin Sodium Salt

β-CD-PO₃Na₂-UCNP-DOX: Doxorubicin Loaded Phosphoric β-Cyclodextrin Stabilized
Upconversion Nanoparticle

β -CD-SO₃Na: Sulfonic β -Cyclodextrin Sodium Salt

β -CD-SO₃Na-UCNP-DOX: Doxorubicin Loaded Sulfonic β -Cyclodextrin Stabilized
Upconversion Nanoparticle

γ -CD: γ -Cyclodextrin

γ -CD-COONa: Carboxylic γ -Cyclodextrin Sodium Salt

γ -CD-COOH-UCNP-DOX: Doxorubicin Loaded Carboxylic γ -Cyclodextrin Stabilized
Upconversion Nanoparticle